ChemPubSoc Europe

DOI: 10.1002/chem.201804166

CHEMISTRY A European Journal Full Paper

Photochemistry

T_1 Population as the Driver of Excited-State Proton-Transfer in 2-Thiopyridone

Sebastian Eckert,*[a] Jesper Norell,*[b] Raphael M. Jay,[a] Mattis Fondell,[c] Rolf Mitzner,[c] Michael Odelius,[b] and Alexander Föhlisch[a, c]

Abstract: Excited-state proton transfer (ESPT) is a fundamental process in biomolecular photochemistry, but its underlying mediators often evade direct observation. We identify a distinct pathway for ESPT in aqueous 2-thiopyridone, by employing transient N 1s X-ray absorption spectroscopy and multi-configurational spectrum simulations. Photoexcitations to the singlet S_2 and S_4 states both relax promptly through intersystem crossing to the triplet T_1 state. The T_1 state, through its rapid population and near nanosecond lifetime, mediates nitrogen site deprotonation by ESPT in a secondary intersystem crossing to the S_0 potential energy surface. This conclusively establishes a dominant ESPT pathway for the system in aqueous solution, which is also compatible with previous measurements in acetonitrile. Thereby, the hitherto open questions of the pathway for ESPT in the compound, including its possible dependence on excitation wavelength and choice of solvent, are resolved.

Introduction

Protonation and deprotonation of active atomic sites in biomolecular systems crucially define the function and activity of individual building blocks in the hydrogen-bonding network of aqueous environments.[1,2] Such intermolecular coordination can be altered through photoexcitations of the system, dependent on the properties of the involved valence excited states along the decay pathways. Solute–solvent interactions can consequently affect the dominant reaction mechanisms in photochemical processes. In particular, excited-state proton transfer (ESPT), an ubiquitous process in biomolecular systems,[3–7] can be strongly dependent on, and is in some cases also mediated by, the surrounding solvent molecules.[5,8] Here, we study the excited-state dynamics of 2-thiopyridone (2-TP) in an aqueous environment. The compound exhibits optically accessible valence excited states, which have been reported to trigger proton transfer between its nitrogen (N) to its sulfur (S) site.[9] A strong solute–solvent interaction is indicated, for example, by a chemical environment dependent N protonation.[10–13]

Three molecular species previously associated with intra- and inter-molecular ESPT in 2-TP are shown in Figure 1: 2-TP, its N to S site proton transferred tautomer 2-mercaptopyridine (2-MP), and the N site deprotonated anion (2-TP$^-$). The dynamics induced by excitation with 266 nm photons at the S_4 resonance of 2-TP (aq) have been investigated by Du et al.[9] with transient Raman vibrational spectroscopy. They identified transient modes of the 2-MP tautomer in its S_0 state on nanosecond timescales and by that categorize 2-TP as an ESPT compound.[9] Recently, we observed signatures of ultrafast deprotonation of the N site of 2-TP (aq) on sub-picosecond timescales upon 400 nm excitation,[14] supporting this categorization. Additionally, Van Kuiken et al.[15] studied the excited-state dynamics of 2-TP in acetonitrile upon S_2 photoexcitation with 400 nm photons using transient S 1s (tender X-ray) NEXAFS, a method

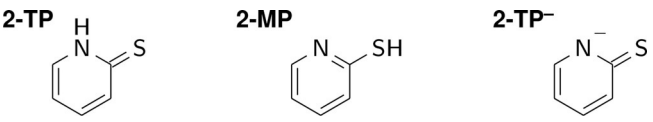

Figure 1. Presently identified molecular species of relevance for ESPT in 2-TP: the thione–thiol tautomers 2-TP and 2-MP, and the deprotonated anion 2-TP$^-$.

[a] S. Eckert, R. M. Jay, Prof. Dr. A. Föhlisch
Institut für Physik und Astronomie
Universität Potsdam, Karl-Liebknecht-Straße 24/25
14476 Potsdam (Germany)
E-mail: sebeckert@uni-potsdam.de

[b] J. Norell, Prof. Dr. M. Odelius
Department of Physics
Stockholm University, AlbaNova University Centre
10691 Stockholm (Sweden)
E-mail: jesper.norell@fysik.su.se

[c] Dr. M. Fondell, Dr. R. Mitzner, Prof. Dr. A. Föhlisch
Institute for Methods and Instrumentation for
Synchrotron Radiation Research
Helmholtz-Zentrum für Materialien und Energie GmbH
Albert-Einstein-Straße 15, 12489 Berlin (Germany)

Supporting information and the ORCID identification number(s) for the author(s) of this article can be found under:
https://doi.org/10.1002/chem.201804166.

proven to yield detailed information on photoinduced dynamics of sulfur-containing molecules.[16,17] Van Kuiken et al.[15] found indications of a transition between the T_1 states of the 2-TP and 2-MP species on sub-ns timescales, but a distinct signature of a N site deprotonated species in its S_0 state was not observed. The mentioned studies differ in terms of excitation energies and solvent environment and have so far not provided a mechanistic understanding of the ESPT in 2-TP.

In this study, we investigate the potentially different, excitation wavelength and solvent dependent, preferential decay pathways of photoexcited 2-TP in solution and identify the relevant transient states of 2-TP mediating the ESPT process. We use N 1s near edge (soft) X-ray absorption fine structure (NEXAFS) spectroscopy, which has proven to be sensitive to N site protonation states[13,14,18–20] and to the valence excited-state dynamics of 2-TP,[14] in an optical pump X-ray probe experimental scheme. Together with spectrum simulations and energy levels from high-level multi-configurational quantum chemistry, this allows us to identify the molecular species and electronic states involved in the photoinduced decay cascade on pico- to nanosecond timescales. We investigate the response of 2-TP (aq) to both direct S_2 and S_4 photoexcitation on the timescale of sub-nanoseconds to tens of nanoseconds and reevaluate the partially contradictory results in the previous studies. From careful theoretical analysis of available time-resolved spectroscopic data, we put forward a fully consistent interpretation of the pico- to nanosecond decay pathway following photoexcitation of 2-TP involving a transient proton transfer process, which is independent both of excitation wavelength and of solvent.

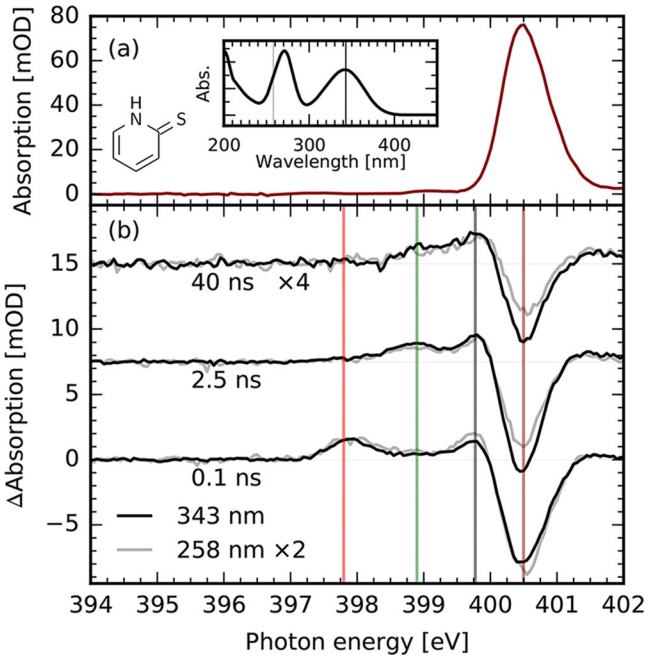

Figure 2. N 1s NEXAFS signatures of excited-state dynamics of aqueous 2-thiopyridone (2-TP, aq) upon 343 nm and 258 nm excitation. (a) Ground-state NEXAFS of 2-TP (aq) exhibiting a distinct π^*-absorption resonance at a photon energy of 400.5 eV. Inset: UV/Vis spectrum of 2-TP (aq) exhibiting S_2 and S_4 resonances excitable with the wavelengths 343 nm and 258 nm (vertical lines). (b) Transient spectra at different (representatively selected) optical pump–X-ray probe delays. The spectra for both excitation wavelengths exhibit the same transient features: a bleach of the main absorption line at 400.5 eV (marked in dark red) and an absorption increase at 399.8 eV (gray), which are present for all studied delays; an absorption resonance at 397.8 eV (red) for 0.1 ns delay, which is replaced by a resonance at 398.9 eV (green) at 2.5 ns delay. The transient spectra are offset vertically for visibility.

Results and Discussion

The N 1s NEXAFS spectrum of 2-TP (aq) shown in Figure 2a exhibits a distinct π^*-resonance at a photon energy of 400.5 eV, assigned to excitation into the $5\pi^*$ LUMO. For the transient spectra, we focus on intensity changes for photon energies below and on this resonance, to avoid spectral overlap with continuum contributions in the analysis. The marked excitation wavelengths in the UV/Vis spectrum of the sample, presented in the inset in Figure 2a, confirm that the two distinct optical absorption resonances are driven dominantly under the experimental conditions. In accordance with Du et al.,[9] our electronic structure calculations show that the lowest valence excited states of 2-TP can be grouped into singlet/triplet—pairs of identical $n\rightarrow\pi^*$ or $\pi\rightarrow\pi^*$ excitation character, as shown in Table 1. In detail, these correspond to electronic excitations from the 4π HOMO (S_2/T_1 and S_4) and the S site lone-pair $14\sigma^n$ HOMO-1 (S_1/T_2 and S_3) into the $5\pi^*$ LUMO (S_1/T_2 and S_2/T_1) and $6\pi^*$ LUMO + 1 (S_3 and S_4). Hence, the two optical absorption resonances in the UV/Vis spectrum correspond to $\pi\rightarrow\pi^*$ excitations to the S_2 and S_4 states, whereas excitation out of the lone-pair orbital and to triplet states are optically dark.

The transient NEXAFS spectra in an energy range between 394 eV and 402 eV at different pump-probe delays are presented in Figure 2b. The displayed spectra for the two different excitation wavelengths exhibit the same transient signatures in the investigated range of pump-probe delays from 0.1 ns to 40 ns. This indicates that the decay pathways from the S_2 and the S_4 valence excited states of 2-TP (aq) merge at a common intermediate (excited state) on or below a picosecond timescale, with indistinguishable subsequent kinetics. The de-

Table 1. Relative energies (in eV) of the electronic states of the molecular species in aqueous solution, in the Franck–Condon (FC) region of the optical pump-excitation and in their relaxed (R) structures.

State[a]	2-TP$_{FC}$	2-TP$_R$	2-MP$_R$	2-TP^-_R
S_0	0.00	0.00	0.58	0.00[b]
S_1 (n, π^*)	3.87	2.94	5.38	3.50[b]
S_2 (π, π^*)	3.89	3.15	5.12	3.46[b]
T_1 (π, π^*)	3.16	2.66	4.42	3.20[b]
T_2 (n, π^*)	3.60	2.95	4.85	3.40[b]
S_3 (n, π^*)	5.08	–	–	–
S_4 (π, π^*)	5.13	–	–	–

[a] States have been enumerated according to their 2-TP energies; states in 2-MP and 2-TP$^-$ are instead denoted to correspond to the same excitation characters as in 2-TP, without consideration of their internal energy ordering. [b] The energies of 2-TP$^-$ have been shifted by −13.44 eV to align 2-TP S_0 and 2-TP$^-$ S_0, as the PCM model cannot be applied to accurately account for interactions of the removed proton with the aqueous solvent surrounding; all presented 2-TP$^-$ energies thereby constitute a lower-bound for the true relative energy.

creased 2-TP S_0 population for positive pump-probe delays causes a bleach (vertical dark red line) of the absorption centered at 400.5 eV. The species present at a delay of 0.1 ns contribute to the first detected transient absorption feature (vertical red line) peaked at 397.8 eV. At a delay of 2.5 ns, a second feature (vertical green line) is picked up at 398.9 eV whereas the first feature at 397.8 eV is no longer present. A third transient feature (vertical gray line) at 399.8 eV (close to the bleach), as well as the bleach itself, are additionally detected at all pump-probe delays up to 40 ns.

We now introduce the framework in which the detected transient NEXAFS signatures will be assigned to electronic states of the three possible molecular species 2-TP, 2-MP, and 2-TP$^-$. Both the simulated spectral contributions and the calculated state energies (for all possible combinations of electronic states and molecular species presented in Figure 3 and Table 1) are considered to identify the observed species through a conclusive process of elimination. As the system relaxing from the initial S_2 and S_4 excitations appears to have reached a common pathway on the investigated timescales, we employ a strict energetic argument: No excited states energetically above 2-TP S_2 are considered as possible detected transient species. The energies of all 2-TP and 2-MP states can be directly related. The energies of 2-TP$^-$ in its different states, however, can neither be directly related to 2-TP nor to 2-MP. The energy of the deprotonation cannot be accurately determined from the simulations, as even if a bare dissociated proton had been included, its covalent bonding with the surrounding solvent molecules would have been neglected by the polarizable continuum model (PCM). The presented energies of 2-TP$^-$ have therefore instead been shifted to align the S_0 state energies of 2-TP and 2-TP$^-$. This shift is well motivated to define a lower bound for the state energies of 2-TP$^-$, as 2-TP is known to be the dominant species over 2-TP$^-$ in a neutral aqueous environment[10–13] (i.e., for the experimental conditions, the energy of 2-TP$^-$ is higher than the energy of 2-TP in the S_0 state).

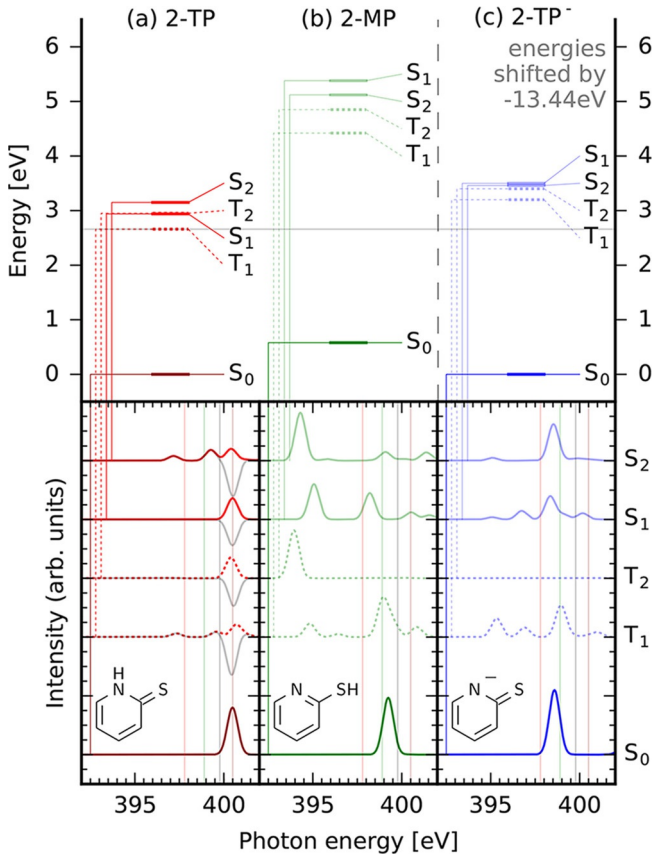

Figure 3. State energies (top) and simulated N 1s NEXAFS spectra (bottom) of 2-thiopyridone (2-TP, a), 2-mercaptopyridine (2-MP, b), and the N site deprotonated anion (2-TP$^-$, c) in the optimized structures of their ground and excited states. Singlet (triplet) states are shown with solid (dashed) lines. The state energies are given relative to the 2-TP S_0 ground state. The gray vertical dashed line separating the simulated state energies of 2-TP$^-$ from the neutral species' highlights the −13.44 eV offset applied to align the energy axes (see text for discussion). Difference spectra are generated by subtraction of the 2-TP S_0 ground-state spectrum for all 2-TP excited-state species (gray lines in a). 2-TP T_1 qualifies as the species present at a delay of 0.1 ns. 2-MP S_0 and 2-TP$^-$ S_0 qualify as one of the species populated at delays between 2.5 and 40 ns. States energetically above 2-TP S_2 (all 2-MP and 2-TP$^-$ excited states) exhibit resonances below 397 eV, which are not detected experimentally, excepting 2-TP$^-$ T_2, which instead shows no intensity in the relevant energy region.

The simulations show that all excited states in 2-MP and 2-TP$^-$ can be excluded as possible detected transient species. Firstly, energetic limitations in the reaction kinetics render them non-accessible from the 2-TP S_2 state (as shown at the top of Figure 3 and in Table 1). Secondly, the associated opening of resonances at photon energies below 397 eV (see Figure 3 b,c) is in contradiction with the transient experimental spectra, even if we allow for some uncertainty in the peak positions associated with the implicit solvation model. The 2-TP S_1 and T_2 states exhibit $n\rightarrow\pi^*$ excitations from an S site lone-pair orbital and consequently do not open any additional N 1s absorption resonances in the regions of the detected transients. Thus, the only two electronically excited species that can be responsible for the first observed transient feature (397.8 eV, red) are the 2-TP S_2 and 2-TP T_1 states, which are associated with $\pi\rightarrow\pi^*$ excitations. The spectrum simulations for these states show that in this system our probe is not directly sensitive to spin degrees of freedom; the two states exhibit virtually identical spectral signatures and must be considered as equally likely candidates from a spectroscopic point of view. Yet, with a lifetime of the excited state in the hundreds of picoseconds, we still assign this transient feature confidently to a dominant (or exclusive) 2-TP T_1 population. This assignment is based on the fact that the T_1 state is the lowest electronically excited state of 2-TP. Such intersystem crossing (ISC) to the triplet state manifold upon photoexcitation has been previously shown to occur on sub-picosecond timescales in similar thione compounds from spectroscopic measurements and simulations of excited-state dynamics.[21–23]

The S_0 ground states of the 2-MP and 2-TP$^-$ species both exhibit a single N 1s π^* resonance at approximately 399 eV in the simulations. This agrees well with the previously determined experimental resonance of 2-TP$^-$,[13,14] and it coincides with the second detected transient feature (398.9 eV, green). As all other combinations of electronic states and molecular species have previously either been ruled out or assigned, the associat-

ed transient species can be conclusively assigned to result from deprotonation of the N site. Owing to the spectral similarities of 2-MP and 2-TP$^-$ in the S_0 state, however, the protonation state of the S site cannot be unambiguously determined, leaving the 2-MP and 2-TP$^-$ molecular species as equally viable candidates.

The third transient feature (399.8 eV, gray) is, as previously noted, present in all spectra at the different pump-probe delays. For the 2-TP T_1 state, the LUMO absorption resonance is slightly shifted with respect to 2-TP S_0, which could yield a low energy shoulder to the ground state bleach. However, as neither 2-MP nor 2-TP$^-$ in their S_0 states exhibit any features in the relevant region, the transient cannot be described by the considered combinations of electronic excitations and molecular species at nanosecond timescales. Owing to its apparent formation upon decay from 2-TP T_1, the transient most likely arises from the release of energy into the surrounding solvent environment upon reformation of 2-TP S_0 (and similarly also for 2-MP/2-TP$^-$ S_0). Such thermalization is known to occur on a timescale of ten picoseconds.[24] The feature is present for tens of nanoseconds after the optical excitation, which is clearly too long for the energy to remain contained within vibrational excitations of the molecule itself. The dissipation of energy into the solvent can thus be expected to appreciably affect the solution as a whole. Laser pump X-ray probe measurements of aqueous solution have shown that the initial isochoric heating leads to significant spectroscopic signatures on nanosecond timescales.[25] The N 1s peak positions are in our case sensitive to solute–solvent interactions.[13] Therefore, it is likely that the relaxation effects on the solvation shell can shift or broaden the spectrum of the 2-TP S_0 state sufficiently to give rise to the transient feature. Such rearrangement of solvent molecules around a photoexcited solute has previously been reported for hard X-ray NEXAFS spectra at the solute absorption edge.[26] This picture is also supported by the increase of the transient intensity at 399.8 eV upon decay of the first transient species within the first nanosecond (see also Figure 4a) as 2-TP in this temperature affected S_0 state can be expected to exhibit a higher absorption cross section close to the ground state π^*-resonance than in the T_1 state. Consequently, we assign the transient to the 2-TP S_0 species in a solvent environment with an increased temperature ("hot" 2-TP S_0), which forms in competition with and subsequently to the N site deprotonated species.

The temporal evolution of the discussed transient spectral signatures is presented in Figure 4. A rate model consisting of the states discussed above and illustrated in Figure 4c was numerically solved and fitted to the data. The contribution of each state at the different energies is given in the Supporting Information. The model yields a lifetime of the 2-TP T_1 state of (0.76 ± 0.05) ns, which decays in a forked pathway to either N site deprotonated 2-MP/TP$^-$ S_0 with a yield of (14 ± 4) %, or the "hot" 2-TP S_0 species with a yield of (86 ± 4) %. The 2-MP/TP$^-$ S_0 species has a lifetime of (7.3 ± 0.3) ns and the "hot" 2-TP S_0 cools down with a time constant of (35 ± 1) ns.

Based on comparison of transient vibrational Raman spectroscopy and quantum chemical simulations, Du et al.[9] identified the presence of 2-MP S_0 at nanosecond scales following S_4 excitation in aqueous solution. No intermediate species were identified; the authors therefore hypothesized three different possible unresolved reaction pathways. This observation is fully consistent with our data, which also supports a deprotonated nitrogen site between roughly 1 to 7 ns. However, as Du et al.[9] did not consider the 2-TP$^-$ species, and we cannot spectrally separate it from 2-MP in the S_0 state in our N 1s edge measurements, it remains undetermined whether an intra-molecular proton transfer occurs directly to the S site or if the proton is fully removed from the molecule into the solvent. Still, our data clearly discriminates between the three proposed pathways, and agrees with the third option proposed by Du et al.,[9] of ESPT through ISC processes through the 2-TP T_1 state. Thus, in extension of their work, we conclusively determine the dominant reaction pathway for proton dynamics in

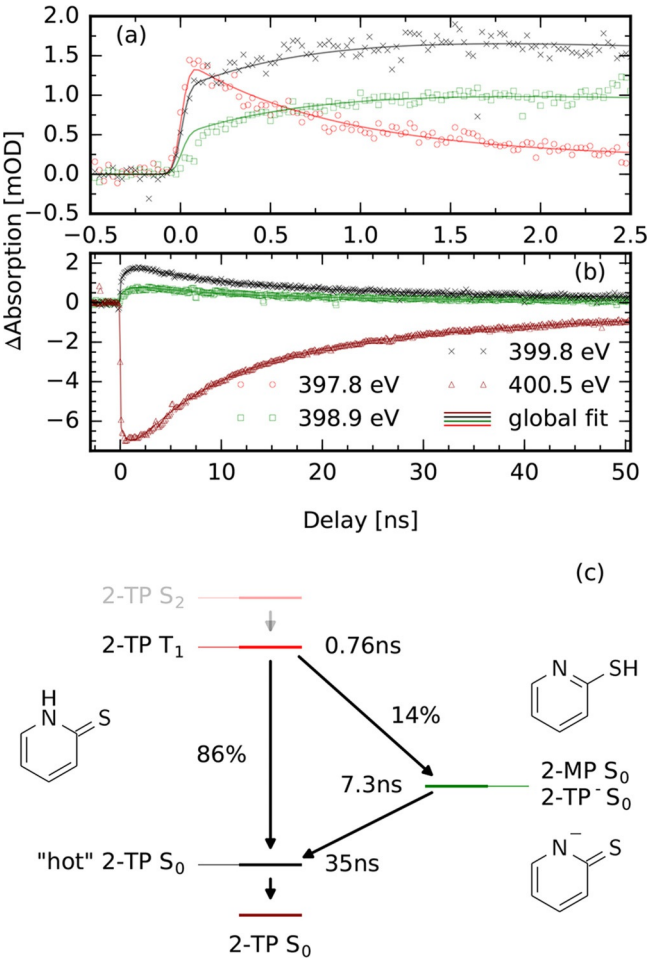

Figure 4. Time traces of selected transients (photon energies marked in Figure 2) for pump-probe delay dependent transient NEXAFS of 2-TP (aq) upon S_2 excitation, with results shown on sub-nanosecond (a) to tens of nanosecond (b) timescales. A rate model described in (c) was fitted to the data set, assuming a decay of the optically accessible singlet states on timescales below our temporal resolution, yielding an initial population of 2-TP T_1 in our experiment, which decays with a lifetime $\tau = (0.76 \pm 0.05)$ ns through a forking into both an N site deprotonated molecular species (2-MP or 2-TP$^-$, $\tau = (7.3 \pm 0.3)$ ns) in its S_0 ground state and a temperature affected "hot" 2-TP S_0 ($\tau = (35 \pm 1)$ ns), with subsequent decay into the 2-TP S_0 state.

2-TP upon S_4 excitation in aqueous solution, and can additionally confirm it to be the same also for S_2 excitation.

Unlike Du et al.,[9] Van Kuiken et al.[15] studied the S_2 photoexcited dynamics of 2-TP in acetonitrile solution. As in the current work, the dynamics were probed with time-resolved NEXAFS spectroscopy, but from the alternative perspective of the S 1s edge. For direct comparison, we have therefore also performed simulations of the transient S 1s NEXAFS spectra of all our considered species as shown in the Supporting Information, which in large part agree with the measurements and DFT simulations by Van Kuiken et al.[15] Similarly to us, Van Kuiken et al.[15] assigned the 2-TP T_1 decay to the formation of the 2-MP molecular species, followed by eventual reformation of 2-TP S_0. However, the authors proposed population of the 2-MP T_1 state as an intermediate from 2-TP T_1 to 2-MP S_0, based on the presence of a transient feature that seemingly overlaps the ground state bleach. As their measurements were performed in acetonitrile, instead of water, the reaction kinetics could in principle differ even qualitatively. Nevertheless, comparison of the state energies in acetonitrile listed in Table S2 in the Supporting Information shows that 2-MP is still 0.6 eV higher in energy than 2-TP in their T_1 states as the relative energy is here not strongly affected by the choice of solvent. An additional activation energy barrier must also be passed in a transition state structure for the transfer to occur on the T_1 potential energy surface. This makes the transition highly unlikely to occur owing to kinetic constraints. As the authors also assign the transient a 15 ns lifetime, it likely corresponds to the signature we assign to "hot" 2-TP S_0. Similarly to our data, the associated S 1s transient feature could in fact be well explained by a temperature-induced broadening and/or shift of the 2-TP S_0 resonance. As further shown in the Supporting Information, S 1s NEXAFS can, analogous to N 1s NEXAFS, hardly distinguish both T_1 from S_2 in 2-TP, and 2-MP from 2-TP$^-$ in the S_0 state, thereby also leaving the initial electronic dynamics and the S site protonation states undetermined. By reasonably reassigning one of the transient species in the interpretation of Van Kuiken et al.,[15] it is thereby fully consistent also with our data and rate model, indicating that the choice of solvent between water and acetonitrile only has a quantitative effect on the timescales of the reaction kinetics.

The proposed pathway for proton transfer in 2-TP results from two steps of ISC, both to and from the T_1 state of 2-TP. The probability for ISC is enhanced in such systems by the presence of the S atom generating an internal heavy atom effect, that is, increased spin-orbit coupling that mixes the spin multiplicities. Originally understood through El-Sayed's rule,[27] ISC in N-heterocyclics is considered more efficient when occurring between states of different excitation character (i.e. (n, π^*) state to (π, π^*) state, or vice-versa), which leaves both $S_2 \rightarrow S_1 \rightarrow T_1$ and $S_2 \rightarrow T_2 \rightarrow T_1$ as probable decay sequences, further facilitated by the small S_1–S_2 and T_1–T_2 energy separations. Alternate and even forked pathways for T_1 population have also been reported.[21,22] Definitive determination of the sub-picosecond dynamics that precedes 2-TP T_1 relaxation will therefore require further investigation with femtosecond spectroscopy methods and simulations of excited-state molecular dynamics.

In contrast to the ultrafast T_1 population, ISC from the T_1 state back to S_0 is clearly a less efficient process, which here occurs on the pico- to nanosecond timescale. This is not surprising considering the S_0–T_1 energy gap of 2.66 eV even in the relaxed T_1 structure, which greatly weakens non-adiabatic coupling to the S_0 surface. The ISC is therefore likely mediated by strong fluctuations in structure and/or solvation. These fluctuations then momentarily bridge the energy gap, and mediate the proton transfer in the non-equilibrium dynamics together with the subsequent release of kinetic energy, before energy dissipation to the solvent can fully return the system to the 2-TP S_0 state in its relaxed structure. It also offers a feasible explanation of our recent measurement with time-resolved resonant inelastic X-ray scattering wherein a signature of N-H dynamics was detected on femtosecond timescales.[14] Within the framework of the dominant relaxation pathway established in this work, a fractional deprotonation can still occur within the timeframe of the relaxation from the photoexcited 2-TP S_2 or S_4 states to 2-TP T_1. As proton transfer is clearly a minority channel, even in the currently proposed pathway, it is thus reasonable that the N–H bond can be affected by the 1.23 eV and 2.47 eV respectively released in the decay from the S_2 and S_4 states in the Franck–Condon region to the relaxed 2-TP T_1. This could activate molecular vibrational modes, for example, an N–H stretch, and yield a forked relaxation pathway with partial N deprotonation as the result. The crucial role of solute–solvent interactions in the proposed proton transfer mechanism would also explain the different reaction rates observed in the two solvents: protic water and aprotic acetonitrile.

Conclusion

The relaxation pathway for excited-state dynamics following S_2 and S_4 excitation of aqueous 2-TP was determined from transient N 1s NEXAFS spectroscopy and multi-configurational spectrum simulations. The pathways populated by the two excitations merge to a common species assigned as 2-TP T_1 on sub-nanosecond timescales. Decay of the T_1 state within roughly a nanosecond results in a forked pathway. This, as majority channel, leads back to the 2-TP S_0 state or, as a minority channel, induces a deprotonation of the N site, that is, an ESPT process. The ESPT yields either the thiol tautomer 2-MP or the N site deprotonated anion 2-TP$^-$, with a lifetime of a few ns. The release of kinetic energy upon electronic de-excitation results in a "hot" solution environment from which the energy fully dissipates on a scale of tens to a hundred ns.

The assigned dominant decay pathway via the 2-TP T_1 state establishes one of three previously proposed, but unresolved, pathways for ESPT. Comparison with S 1s NEXAFS measurements indicate that the same pathway is populated upon 2-TP S_2 excitation also in acetonitrile solution. The assigned photoinduced proton dynamics thus are independent of the choice of excitation wavelength and protic (aqueous) or aprotic (acetonitrile) solvent. The proposed pathway highlights dissipation of kinetic energy in non-equilibrium dynamics as the prime driver of the ESPT in 2-TP, a finding of general applicability in studies of ESPT processes as photo-protection mechanisms in biomol-

ecules. Our results provide the framework for investigations of the initial ultrafast (sub-picosecond) relaxation and further characterization of the observed ESPT as an intra- or inter-molecular process.

Experimental and Computational Section

The aqueous 2-TP solution, prepared at a concentration of 150 mM from 2-mercaptopyridine 99% supplied by Sigma–Aldrich and dissolved in deionized water, was sprayed into the experimental vacuum chamber in a liquid flat jet sample environment. The transmitted average intensity of synchrotron radiation from the beamline UE52-SGM at the synchrotron BESSY II with a bandwidth of 35 meV was monitored using a gallium arsenide photodiode to record the static N 1s NEXAFS of 2-TP. A background generated from the tabulated attenuation length of the chemical composition of the solution without the N contribution was subtracted from the spectrum. The transient changes of the absorption were induced using approximately 300 fs long pulses of the third and fourth harmonic centered at 343 nm and 258 nm of a fiber laser system with a fundamental wavelength of 1030 nm. It was operated at a repetition rate of 208 kHz and the laser beam was focused to a dimension of $(80\times80)\ \mu m^2$ FWHM. The laser system was synchronized with the arrival time of the hybrid bunch in the gap of BESSY II fill pattern and the arrival time was shifted with respect to the arrival time of the X-ray pulses originating from the hybrid bunch to adjust the pump-probe delay. The hybrid bunch provides X-ray probe pulses with a bandwidth of 120 meV at a rate of 1.25 MHz. The intensity of each X-ray pulse accompanied by a laser pulse as well as the pulse intensity 4 μs later, transmitting the replenished sample in its electronic ground state, were recorded from the voltage pulse of a capped (200 nm Al film) silicon avalanche photodiode. The signal was amplified by 20 dB and accumulated using a digital boxcar averager from Zürich Instrument AG. This scheme yields a differential measurement of the transient absorption changes. Details of the measurement scheme have been summarized by Fondell et al.[28] The sample thickness was estimated from the attenuation of the synchrotron radiation by the jet in comparison to tabulated attenuation values[29] to be approximately 6.5 μm for the static spectrum in Figure 2a, 6.3 μm for the transient spectra in Figure 2b, and 3.9 μm for the delay dependent absorption changes in Figure 4 for 343 nm excitation. The spectra for 258 nm excitation were accumulated at sample thicknesses in the few μm range. The pulse energies used for the excitation were 12.4 μJ for the transient spectra at 343 nm, 3.3 μJ for the delay traces at 343 nm, and 2.7 μJ for the spectra at 258 nm. The UV/Vis spectrum of 2-TP (aq) was recorded using a Shimadzu UV-2700 spectrometer at a sample concentration of 0.1 mM in a quartz cuvette, providing a 10 mm sample thickness.

Multi-configurational quantum chemical calculations were performed with the complete active space self-consistent field (CASSCF)[30] method, restricted active space self-consistent field (RASSCF)[31] method, and the second-order perturbation theory restricted active space (RASPT2)[32] multi-state[33] method, with the 6-31G basis set, as implemented in the Molcas 8.2 program package.[34] No explicit use of symmetry was employed for geometry optimization nor for the electronic structure calculations.

Geometry optimization of all molecular species (i.e., molecular structures and electronic states) was performed at the CASSCF(10,8) level (10 electrons in 8 orbitals), with an active space that included the initially occupied $4\times\pi$ orbitals, the initially occupied $1\times\sigma$ lone-pair orbital (S centered in 2-TP and 2-TP$^-$, N centered in 2-MP), and the initially unoccupied $3\times\pi^*$ orbitals.

Spectrum simulations were performed with RASSCF calculations and subsequent application of multi-state RASPT2, the latter utilizing an imaginary shift of 0.05 Hartree to accelerate convergence. Interactions with the aqueous surrounding were approximately included through a polarizable continuum model (PCM) equilibrated to the initial state of NEXAFS process.[35] The active space included the same orbitals in the RAS2 space (no restrictions, equivalent to the complete active space method) as in the corresponding geometry optimization and, additionally, the N 1s core orbital in the RAS1 space (restricted to a maximum of one electron-hole). The N 1s orbital was frozen for the RASSCF orbital optimization, to avoid relaxation from core- to valence-excitations in the final state calculations. For each spectrum, five (three for 2-MP owing to convergence problems of the higher states) non-core-excited states (ground state and valence-excited) and ten core-excited states, were separately obtained within the state averaging formalism. Core-excited states were obtained through a separate orbital constraint on the N 1s orbital (to avoid rotation with N 2s) and the highly excited states (HEXS) method[36] (which eliminates contributions for all electronic configurations with doubly occupied N 1s). Transition electronic dipole moments for NEXAFS intensities were obtained with the RAS state interaction method (RASSI).[37,38] For comparison with the measured NEXAFS spectra, the simulated discrete transitions were convoluted with a Gaussian broadening of 0.7 eV accounting for the bandwidth of incident radiation in combination with inhomogeneity and dynamical effects in the sample through solute–solvent interactions. The Lorentzian lifetime broadening with full-width at half-maximum (FWHM) was neglected (estimated as 0.11 eV[39] from N_2 and N_2O). An absolute shift of −3.78 eV (to account for, for example, the frozen N 1s orbital and limitations in dynamical correlation) was applied to the energies of all core-excited states, which aligns the absorption resonance of 2-TP S_0 to the experimental value of 400.5 eV.

Acknowledgments

We thank HZB for the allocation of synchrotron radiation beamtime. We thank Christian Weniger, Ruslan Ovsyannikov, and Daniel Schick for technical support during the measurements. S.E., R.M.J., and A.F. acknowledge funding from the ERC-ADG-2014—Advanced Investigator Grant No. 669531 EDAX under the Horizon 2020 EU Framework Programme for Research and Innovation. M.O. acknowledges financial support

from the Swedish Research Council (VR) (contract number 2015-03956). M.O. and J.N. acknowledge financial support from the Helmholtz Virtual Institute VI 419 "Dynamic Pathways in Multidimensional Landscapes". The quantum chemical calculations were partially performed with resources provided by the Swedish National Infrastructure for Computing (SNIC) at the Swedish National Supercomputer Center (NSC), the High-Performance Computer Center North (HPC2N), and Chalmers Centre for Computational Science and Engineering (C3SE).

Conflict of interest

The authors declare no conflict of interest.

Keywords: excited-state proton-transfer · intersystem crossing · nitrogen · photochemistry · X-ray absorption

[1] A. Warshel, *Acc. Chem. Res.* **1981**, *14*, 284 – 290.
[2] M. Perutz, *Science* **1978**, *201*, 1187 – 1191.
[3] T. Schultz, E. Samoylova, W. Radloff, I. V. Hertel, A. L. Sobolewski, W. Domcke, *Science* **2004**, *306*, 1765 – 1768.
[4] Y. Zhang, K. de La Harpe, A. A. Beckstead, R. Improta, B. Kohler, *J. Am. Chem. Soc.* **2015**, *137*, 7059 – 7062.
[5] A. Corani, A. Pezzella, T. Pascher, T. Gustavsson, D. Markovitsi, A. Huijser, M. D'Ischia, V. Sundström, *J. Phys. Chem. Lett.* **2013**, *4*, 1383 – 1388.
[6] A. Corani, A. Huijser, T. Gustavsson, D. Markovitsi, P. Å. Malmqvist, A. Pezzella, M. D'Ischia, V. Sundström, *J. Am. Chem. Soc.* **2014**, *136*, 11626 – 11635.
[7] A. El Nahhas, T. Pascher, L. Leone, L. Panzella, A. Napolitano, V. Sundström, *J. Phys. Chem. Lett.* **2014**, *5*, 2094 – 2100.
[8] S. Banerjee, A. Pabbathi, M. C. Sekhar, A. Samanta, *J. Phys. Chem. A* **2011**, *115*, 9217 – 9225.
[9] R. Du, C. Liu, Y. Zhao, K.-M. Pei, H.-G. Wang, X. Zheng, M. Li, J.-D. Xue, D. L. Phillips, *J. Phys. Chem. B* **2011**, *115*, 8266 – 8277.
[10] P. Beak, *Acc. Chem. Res.* **1977**, *10*, 186 – 192.
[11] P. Beak, J. B. Covington, *J. Am. Chem. Soc.* **1978**, *100*, 3961 – 3963.
[12] P. Beak, J. B. Covington, S. G. Smith, J. M. White, J. M. Zeigler, *J. Org. Chem.* **1980**, *45*, 1354 – 1362.
[13] S. Eckert, P. Miedema, W. Quevedo, B. O'Cinneide, M. Fondell, M. Beye, A. Pietzsch, M. Ross, M. Khalil, A. Föhlisch, *Chem. Phys. Lett.* **2016**, *647*, 103 – 106.
[14] S. Eckert, J. Norell, P. S. Miedema, M. Beye, M. Fondell, W. Quevedo, B. Kennedy, M. Hantschmann, A. Pietzsch, B. E. Van Kuiken, M. Ross, M. P. Minitti, S. P. Moeller, W. F. Schlotter, M. Khalil, M. Odelius, A. Foehlisch, *Angew. Chem. Int. Ed.* **2017**, *56*, 6088 – 6092; *Angew. Chem.* **2017**, *129*, 6184 – 6188.
[15] B. E. Van Kuiken, M. R. Ross, M. L. Strader, A. A. Cordones, H. Cho, J. H. Lee, R. W. Schoenlein, M. Khalil, *Struct. Dyn.* **2017**, *4*, 044021.
[16] M. Ochmann, I. von Ahnen, A. A. Cordones, A. Hussain, J. H. Lee, K. Hong, K. Adamczyk, O. Vendrell, T. K. Kim, R. W. Schoenlein, N. Huse, *J. Am. Chem. Soc.* **2017**, *139*, 4797 – 4804.
[17] M. Ochmann, A. Hussain, I. von Ahnen, A. A. Cordones, K. Hong, J. H. Lee, R. Ma, K. Adamczyk, T. K. Kim, R. W. Schoenlein, O. Vendrell, N. Huse, *J. Am. Chem. Soc.* **2018**, *140*, 6554 – 6561.
[18] M. Blum, M. Odelius, L. Weinhardt, S. Pookpanratana, M. Bär, Y. Zhang, O. Fuchs, W. Yang, E. Umbach, C. Heske, *J. Phys. Chem. B* **2012**, *116*, 13757 – 13764.
[19] M. Ekimova, W. Quevedo, Ł. Szyc, M. Iannuzzi, P. Wernet, M. Odelius, E. T. J. Nibbering, *J. Am. Chem. Soc.* **2017**, *139*, 12773 – 12783.
[20] S. Eckert, J. Niskanen, R. M. Jay, P. S. Miedema, M. Fondell, B. Kennedy, W. Quevedo, M. Iannuzzi, A. Föhlisch, *Phys. Chem. Chem. Phys.* **2017**, *19*, 32091 – 32098.
[21] S. Mai, M. Pollum, L. Martínez-Fernández, N. Dunn, P. Marquetand, I. Corral, C. E. Crespo-Hernández, L. González, *Nat. Commun.* **2016**, *7*, 13077.
[22] S. Mai, P. Marquetand, L. González, *J. Phys. Chem. Lett.* **2016**, *7*, 1978 – 1983.
[23] M. Pollum, S. Jockusch, C. E. Crespo-Hernández, *Phys. Chem. Chem. Phys.* **2015**, *17*, 27851 – 27861.
[24] J. Ojeda, C. A. Arrell, L. Longetti, M. Chergui, J. Helbing, *Phys. Chem. Chem. Phys.* **2017**, *19*, 17052 – 17062.
[25] N. Huse, H. Wen, D. Nordlund, E. Szilagyi, D. Daranciang, T. A. Miller, A. Nilsson, R. W. Schoenlein, A. M. Lindenberg, *Phys. Chem. Chem. Phys.* **2009**, *11*, 3951 – 3957.
[26] V.-T. Pham, W. Gawelda, Y. Zaushitsyn, M. Kaiser, D. Grolimund, S. L. Johnson, R. Abela, C. Bressler, M. Chergui, *J. Am. Chem. Soc.* **2007**, *129*, 1530 – 1531.
[27] M. A. El-Sayed, *J. Chem. Phys.* **1963**, *38*, 2834 – 2838.
[28] M. Fondell, S. Eckert, R. M. Jay, C. Weniger, W. Quevedo, J. Niskanen, B. Kennedy, F. Sorgenfrei, D. Schick, E. Giangrisostomi, R. Ovsyannikov, K. Adamczyk, N. Huse, P. Wernet, R. Mitzner, A. Föhlisch, *Struct. Dyn.* **2017**, *4*, 054902.
[29] B. Henke, E. Gullikson, J. Davis, *At. Data Nucl. Data Tables* **1993**, *54*, 181 – 342.
[30] B. O. Roos, P. R. Taylor, P. E. Siegbahn, *Chem. Phys.* **1980**, *48*, 157 – 173.
[31] P.-Å. Malmqvist, A. Rendell, B. O. Roos, *J. Phys. Chem.* **1990**, *94*, 5477 – 5482.
[32] P.-Å. Malmqvist, K. Pierloot, A. R. M. Shahi, C. J. Cramer, L. Gagliardi, *J. Chem. Phys.* **2008**, *128*, 204109.
[33] J. Finley, P.-Å. Malmqvist, B. O. Roos, L. Serrano-Andrés, *Chem. Phys. Lett.* **1998**, *288*, 299 – 306.
[34] F. Aquilante, J. Autschbach, R. K. Carlson, L. F. Chibotaru, M. G. Delcey, L. De Vico, I. F. Galván, N. Ferré, L. M. Frutos, L. Gagliardi, M. Garavelli, A. Giussani, C. E. Hoyer, G. L. Manni, H. Lischka, D. Ma, P. Å. Malmqvist, T. Müller, A. Nenov, M. Olivucci, T. B. Pedersen, D. Peng, F. Plasser, B. Pritchard, M. Reiher, I. Rivalta, I. Schapiro, J. Segarra-Martí, M. Stenrup, D. G. Truhlar, L. Ungur, A. Valentini, S. Vancoillie, V. Veryazov, V. P. Vysotskiy, O. Weingart, F. Zapata, R. Lindh, *J. Comput. Chem.* **2016**, *37*, 506 – 541.
[35] M. Cossi, V. Barone, *J. Chem. Phys.* **2000**, *112*, 2427 – 2435.
[36] M. Guo, L. K. Sørensen, M. G. Delcey, R. V. Pinjari, M. Lundberg, *Phys. Chem. Chem. Phys.* **2016**, *18*, 3250 – 3259.
[37] P.-Å. Malmqvist, B. O. Roos, *Chem. Phys. Lett.* **1989**, *155*, 189 – 194.
[38] P.-Å. Malmqvist, B. O. Roos, B. Schimmelpfennig, *Chem. Phys. Lett.* **2002**, *357*, 230 – 240.
[39] K. C. Prince, M. Vondrácek, J. Karvonen, M. Coreno, R. Camilloni, L. Avaldi, M. de Simone, *J. Electron Spectrosc. Relat. Phenom.* **1999**, *101*, 141 – 147.

Manuscript received: August 15, 2018
Accepted manuscript online: November 19, 2018
Version of record online: January 8, 2019

